A SYNCHRONIZATION METHOD FOR DOUBLY FED ASYNCHRONOUS GENERATORS FOR WIND POWER SYSTEMS

[1]Helio Voltolini, [2]Thiago Bazzo, [3]Renato Carlson, [4]Nelson J. Batistela, [5]Patrick Kuo-Peng
[1]UTFPR – [2,3,4,5]GRUCAD/UFSC
[1]Ponta Grossa - PR, [2,3,4,5]Florianopolis – SC, BRAZIL
[1]helio@grucad.ufsc.br, [2]bazzo@grucad.ufsc.br, [3]rcarlson@ieee.org, [4]jhoe@grucad.ufsc.br, [5]patrick@grucad.ufsc.br

***Abstract* – In this paper the vector control of the DFIG using a rotating reference frame fixed on the stator flux was implemented in Matlab/Simulink/SymPowerSystems as well as experimentaly. It has been shown that the control algorithm of the grid-side and rotor-side converters can control the active and reactive power independently. The measure of the stator flux angle, realized using a PLL, showed good performance during the system startup. The PLL implemented in the control system has demonstrated a robust behavior under noisy voltage and current signals. A synchronization strategy is proposed where the amplitude, frequency and phase of the stator winding and grid voltages ensures the conditions for a smooth connection by acting in rotor current control loops. Soft and fast synchronization is achieved. Experimental results are presented.**

***Keywords* – doubly-fed, induction generator, synchronization, wind.**

I. INTRODUCTION

Doubly fed induction machines with a wounded rotor have been used as variable speed electric generator especially in wind power generator systems and is known as Doubly Fed Induction Generator (DFIG) [1],[2]. The stator winding is connected directly to the electrical grid and the rotor winding is connected to a bi-directional static power converter through slip-ring and then to the electrical grid. A general scheme of the DFIG system is shown in Fig. 1 where the subscript ‘s’ stands for ‘stator winding’, subscript ‘r’ for ‘rotor winding’, subscript ‘conv’ for ‘grid-side converter’ and subscript ‘g’ for ‘grid’. The converter power rating is a fraction of that of the electrical machine. This power converter provides to the DFIG the ability to control the active and reactive power flow in the stator winding and consequently in the grid. Due to a bi-directional PWM power converter in the rotor circuit, the DFIG is able to work as a generator in subsynchronous and supersynchronous speed. In wind power applications, the power converter adjusts continuously the generator speed such that the wind turbine operates at maximum power for all wind speeds.

The vector control technique applied to the power converters allows controlling the active and reactive power based in the concept of dq orthogonal reference frame. The vector control based on the stator flux orientation is well documented in the literature and has been applied in industrial applications.

Very few references exist on the synchronization process of doubly-fed induction generators [3-5]. A method to synchronize the induction generator to the grid is presented here that exploits the large capacity of the microprocessor that already controls the PWM converters.

This paper presents an analysis of the DFIG’s vector control based on simulated results with Matlab/Simulink/SymPowerSystem and on experimental results. Dynamic results of the control algorithm and grid synchronization process are presented. An experimental setup using a control board based on a Hitachi SH7047 microprocessor was developed. The laboratory prototype consists of a 3kW, 380V, 60Hz wound rotor asynchronous machine and a WEG back-to-back PWM converter.

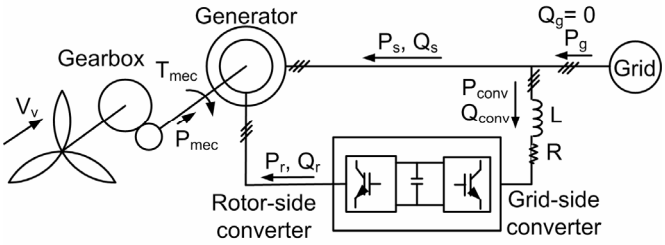

Fig. 1. Representation of the power flow in the system using a ‘motor’ convention.

II. THE GRID-SIDE CONVERTER

The grid-side PWM voltage fed converter is connected to the grid through three single-phase chokes. With this configuration it is possible to operate using boost mode and have attractive features as constant DC bus voltage, low harmonic distortion of grid current, bidirectional power flow and adjustable power factor. The main objective of the grid-side converter is to keep the DC-link voltage constant regardless the magnitude and direction of the rotor winding power. However, it can also be involved in the power factor regulation.

The grid-side converter control, shown in Fig. 2, is based on the dq voltage equations of the grid-reactance-converter system expressed as:

$$\left.\begin{aligned} v_{qe} &= \mathrm{R}i_{qe} + \mathrm{L}\frac{di_{qe}}{dt} + \omega_e \mathrm{L}i_{de} + v_{q1} \\ v_{de} &= \mathrm{R}i_{de} + \mathrm{L}\frac{di_{de}}{dt} - \omega_e \mathrm{L}i_{qe} + v_{d1} \end{aligned}\right\} \quad (1)$$

where L and R are the inductance and resistance of the chokes, respectively, v_{qe}, v_{de}, i_{qe}, i_{de} are the electrical grid voltages and currents in the dq reference frame, v_{q1} and v_{d1} are the AC side voltages of the converter in dq reference frame and ω_e is the angular frequency of the electrical grid. The vector control approach is used, with a reference frame

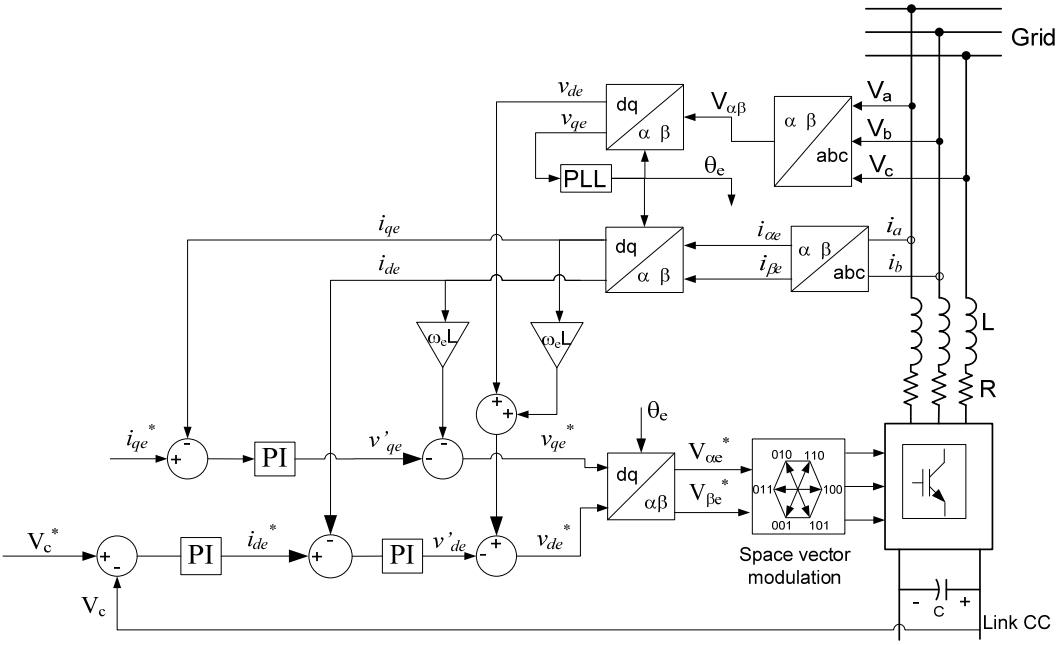

Fig. 2. Control system for the grid-side converter.

oriented along the grid voltage vector (V_e) position, such that v_{de}= V_e and v_{qe}=0. This allows independent control of the active and reactive power through i_{de} and i_{qe}, respectively according to following equations:

$$\left.\begin{aligned} P_e &= \frac{3}{2} V_e i_{de} \\ Q_e &= -\frac{3}{2} V_e i_{qe} \end{aligned}\right\} \qquad (2)$$

The DC link voltage can be controlled for the active power flow between the two converters above the peak value of the grid voltage. In this work the DC link voltage was regulated to 620V for a grid voltage of 380V. Fig. 2 shows the scheme of the grid-side converter and its controls as simulated in Matlab/Simulink/SimPower Systems.

III. ROTOR-SIDE CONVERTER

The vector control of the rotor-side converter is represented in block diagram in Fig. 3. The voltage and current acquisitions are realized with transformers and Hall

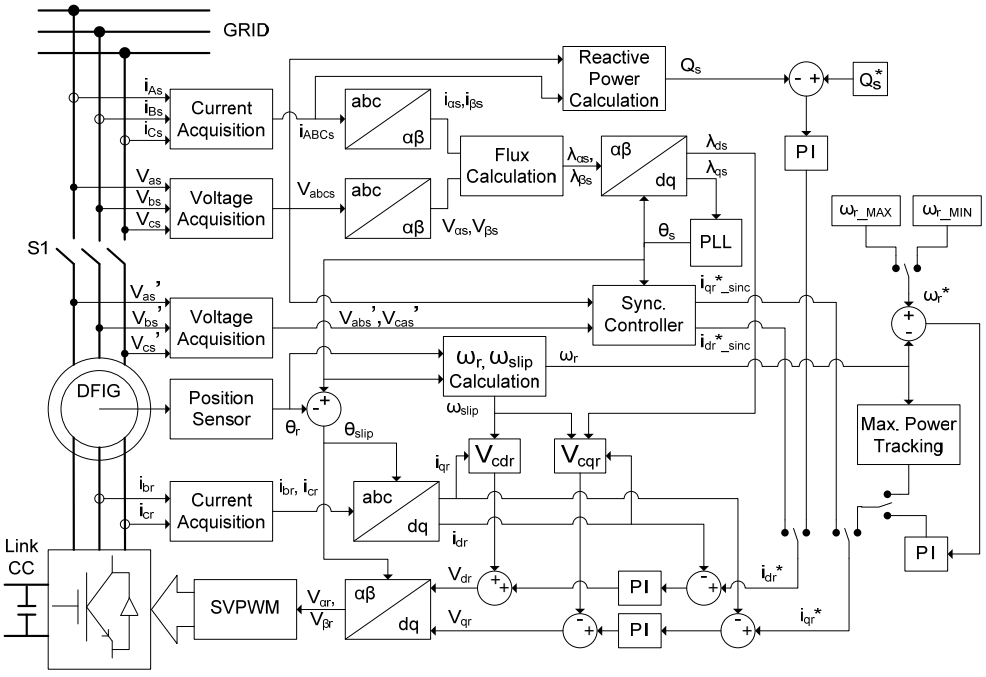

Fig. 3. Rotor-side converter control strategy block diagram.

Effect sensors, respectively. The analog signals are filtered and their levels are adjusted for the analog digital converter located in control board based on the Hitachi SH7047 microprocessor.

The control of the reactive power is realized by acting over the rotor current i_{dr}. The reference current is given by a PI controller that adjusts the reactive power to a desired amount (e.g. $Q_s^* = 0$).

Similarly, the control of the active power is realized by acting over the rotor current i_{qr}. There are three possible situations for defining the current reference in this case. Two of them require a PI controller and correspond to the two speed limits: the maximum and minimum rotating speed. The third one corresponds to track the maximum turbine power for each wind speed.

Fig. 4 shows how the PI current controllers respond to step changes in i_{dr}^* and i_{qr}^*. The controller's response is very fast. However, both controllers show an excessive overshooting (20% on i_{dr}) but this is not really a problem since in this case the reference signals i_{dr}^* and i_{qr}^* come from slower PI controllers.

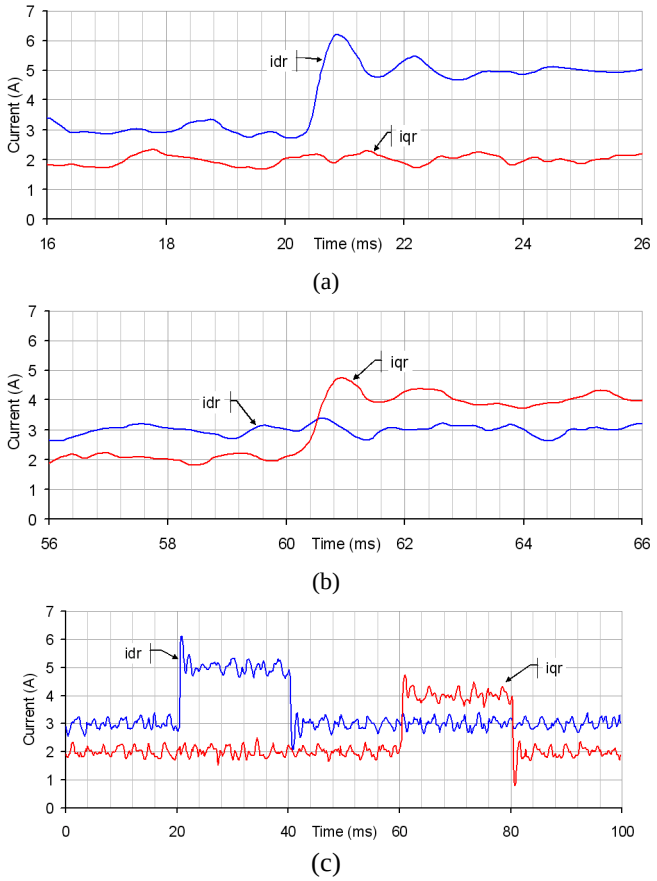

Fig. 4. Experimental i_{dr} and i_{qr} PI control loops response to a step variation: (a) of the direct axis rotor current reference, (b) of the quadrature axis rotor current reference and (c) up and down steps on both currents references at different instants of time.

IV. STATOR FLUX ESTIMATION

The aim of the rotor-side converter is to impose a current to the rotor winding and to control independently the active and reactive power in the stator winding.

After the acquisition, the stator abc voltages and currents are transformed into a stationary αβ coordinate system. Due to delta-star connection of the stator-rotor windings, the voltage $V_{\alpha s}$ is aligned with the line-to-line voltage V_{abs}. Then, the αβ stator voltages and currents are calculated as:

$$\left.\begin{aligned} V_{\alpha s} &= V_{abs} \\ V_{\beta s} &= -\frac{\sqrt{3}}{3}\left(V_{abs} + 2V_{cas}\right) \end{aligned}\right\} \tag{3}$$

$$\left.\begin{aligned} i_{\alpha s} &= \frac{1}{2}\left(i_{As} + i_{Bs}\right) \\ V_{\beta s} &= -\frac{\sqrt{3}}{6}\left(i_{As} + i_{Bs} - 2i_{Cs}\right) \end{aligned}\right\} \tag{4}$$

The stator flux is calculated in the stationary αβ and rotating dq axes as:

$$\left.\begin{aligned} \lambda_{\alpha s} &= \int \left(V_{\alpha s} - \mathrm{r_s} i_{\alpha s}\right) dt \\ \lambda_{\beta s} &= \int \left(V_{\beta s} - \mathrm{r_s} i_{\beta s}\right) dt \end{aligned}\right\} \tag{5}$$

$$\left.\begin{aligned} \lambda_{ds} &= \lambda_{\alpha s}\cos\left(\theta_s\right) + \lambda_{\beta s}\sin\left(\theta_s\right) \\ \lambda_{qs} &= -\lambda_{\alpha s}\sin\left(\theta_s\right) + \lambda_{\beta s}\cos\left(\theta_s\right) \end{aligned}\right\} \tag{6}$$

Fig. 5 shows the block diagram of the αβ/dq transformation and a phase locked loop (PLL) used for stator flux angle estimation. In resume, the PLL provides the stator flux angle such that the d-axis is aligned with total stator winding flux λ_s, i.e., $\lambda_{ds}=\lambda_s$ and $\lambda_{qs}=0$. In order to set the initial condition of integration block the constant ω_e (angular grid frequency) is added after the PI controller. [6]

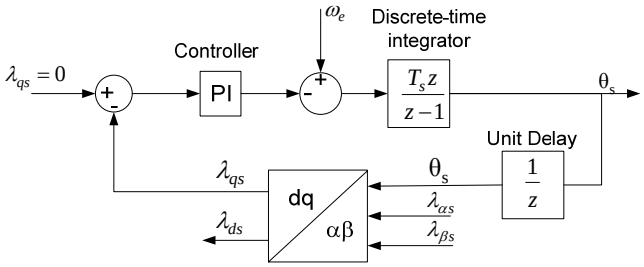

Fig. 5. PLL stator flux angle estimation.

The dynamic performance of the PLL during the startup system is shown in Fig. 6. This result shows that, at the startup system, the flux position operating point is reached in approximately 0.1s. This flux angle estimator strategy has demonstrated a good performance even in the presence of noise in the voltage and current acquisition.

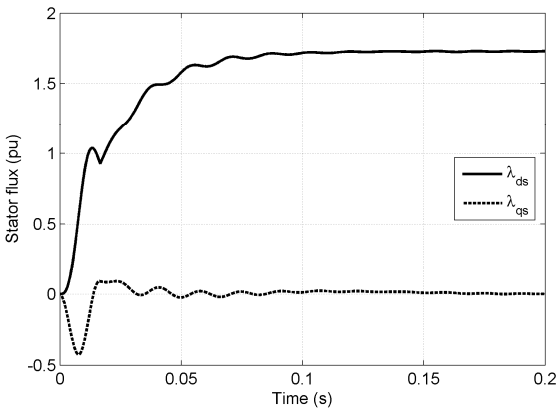

Fig. 6 Simulated stator flux in dq orthogonal reference frame (1 pu= 0.82 Wb)

V. SYNCHRONIZATION TO THE GRID STRATEGY

Previous works on synchronization techniques for the DFIG are quite superficial not presenting a detailed analysis of the adopted synchronization strategy [3-5].

In [3] a matrix converter is used and the synchronization procedure only can be started when the rotor attains the synchronous speed. In this paper, no simulation or experimental results of the synchronization process are presented.

A stator flux oriented vector control is adopted in [4] and the synchronization can be realized at the cut-in wind speed. In this paper, also, no simulation or experimental results of the synchronization process are presented.

In [5] a stator flux oriented vector control is adopted and the synchronization procedure only can be started when the rotor attains the synchronous speed. In this paper, only simulation results of the synchronization process are presented.

In this paper, the grid connection is started as soon as the machine shaft speed reaches the minimum operating value. A soft connection of the generator to the grid is obtained when the phase, frequency and amplitude of the stator and grid voltages are equal before the switch S1 of Fig. 3 is closed.

The block diagram in Fig. 7 shows how the synchronization of the stator winding and grid voltages algorithm was implemented.

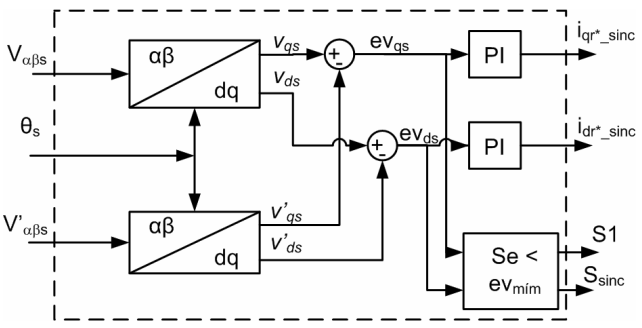

Fig. 7. Block diagram of the synchronization controller.

To start synchronizing the generator with the grid, the rotor winding is fed by the back-to-back converters to create a stator flux and induced voltages. The stator voltages V'_{abs}, V'_{cas} and the grid voltages V_{abs} and V_{cas} are acquired using similar procedures. With the angle θ_s the transformation αβ/dq is applied to both grid and stator voltages. The grid voltages v_{ds} and v_{qs} are compared to the stator voltages v'_{ds} and v'_{qs}. The resulting error is processed by the PI controller that acts over the rotor i_{dr} and i_{qr} current control loops. As the angle used in the grid and stator αβ/dq voltages transformation is the same, equal v_{ds} and v'_{ds} values and equal v_{qs} and v'_{qs} values imply equal phase, frequency and amplitude of the grid and stator winding voltages. In other words, when the error signals of the dq grid and stator winding voltages reaches a small defined value; the synchronism is attained and the system is ready for connection. At this moment (instant t_2 in Fig. 8) a signal is sent by the software to turn on switch S1.

Fig. 8 shows the simulated results of a synchronization process. Signals t_1 and t_2 define the initial and the final instants of the synchronization process, in Fig. 8 they are t_1=2.46 s and t_2 = 2.59 s.

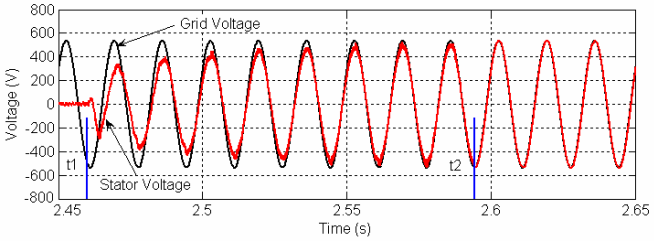

Fig. 8. Simulated results: Stator and grid voltages during the synchronization process that starts at time t1 and ends at time t2.

Fig. 9 shows the experimental results for the synchronization. These two figures show the agreement between simulated and experimental results and, examining the rotor currents, that this process occurs in a smooth way.

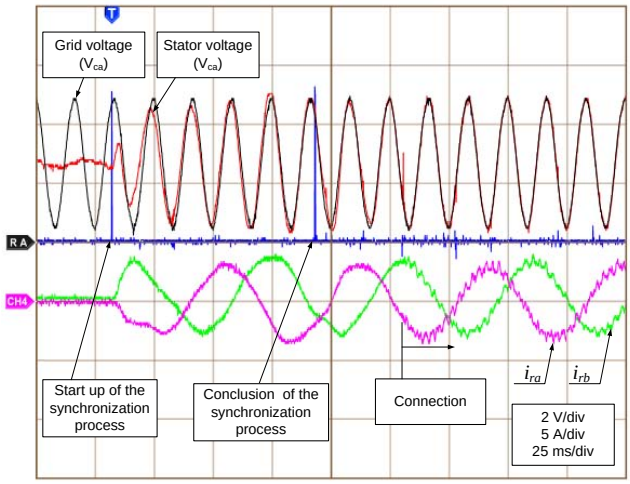

Fig. 9. Experimental results: stator and grid voltages during the synchronization process; i_{ra} and i_{rb} rotor currents during the synchronization process.

The experimental dq voltages of Fig. 7 are shown in Fig. 10 during the synchronization process. In this figure, t_1 corresponds to the start of the synchronization procedure. At time t_2 the grid side and the stator side voltages amplitude, phase and frequency are sufficiently close and the order is

given to switch S1 to close. However, there is a time delay between the instant the order to close is send (t_2) and the instant the switch is effectively closed (t_3).

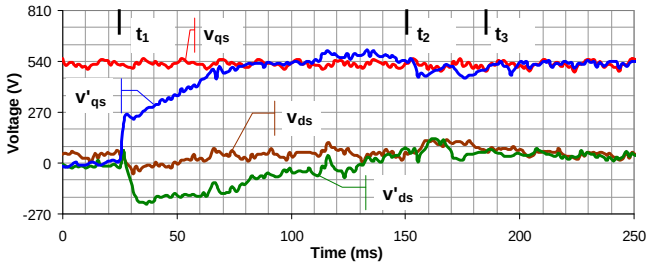

Fig. 10. Experimental dq grid and stator voltages during the synchronization process.

In order to illustrate the behavior of the DFIG, Fig. 11 shows the dq rotor currents including the synchronization procedure as well as the response to an increase of the wind speed.

Before synchronization (t<0.5 s) the rotor currents are obviously null. Immediately after synchronization current i_{dr} increases to the value needed to produce the stator flux linkage that induces the adequate stator voltage.

At t=5 s a step of wind speed occurs increasing the shaft torque and the current i_{qr}. Currents i_{qr} and i_{dr} are proportional to the stator active and reactive power, respectively, as given by Eq. 7. Current i_{dr} keeps constant after synchronization because it corresponds to the value needed to a unity power factor at the grid terminals.

$$\left.\begin{aligned} P_s &= -\frac{3}{2}\frac{L_m}{L_s}\lambda_s\omega_e i_{qr} \\ Q_s &= \frac{3}{2}\left(\frac{\omega_e\lambda_s^2}{L_s} - \frac{L_m}{L_s}\lambda_s\omega_e i_{dr}\right) \end{aligned}\right\} \quad (7)$$

where λ_s is the stator flux, L_m is the magnetizing inductance, L_s is the stator self-inductance and ω_e is the grid frequency.

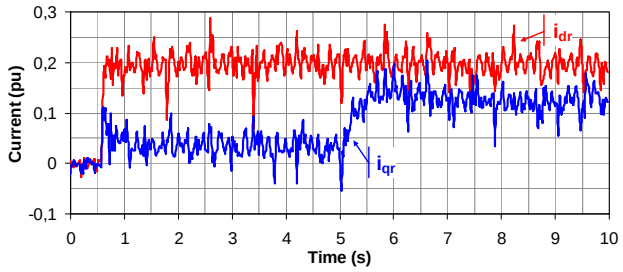

Fig. 11. Experimental dq rotor currents: synchronization occurs at t=0.5 s and a step increase of the wind speed occurs at t= 5 s.

VI. CONCLUSION

In this paper the vector control of the DFIG using a rotating reference frame fixed on the stator flux was implemented in Matlab/Simulink/SymPowerSystems and also on an experimental setup. It has been shown that the control algorithm of the grid-side and rotor-side converters can control the active and reactive power independently.

The simulations of the PLL in order to measure the stator flux angle show good performance during the system startup and its implementation has demonstrated a robust behavior under noisy voltage and current signals.

The proposed synchronization process showed to be fast and smooth. Matching the amplitude, frequency and phase of the stator windings and grid voltages it assures the conditions for the connection by acting over the rotor current control loops.

REFERENCES

[1] R. Pena, J.C. Clare, G.M Asher, “Doubly fed induction generator using back-to-back PWM converter and its application to variable-Speed wind-energy generation.” *IEE Proc.-Electr. Power Appl.*, Vol. 143, No. 3, May 1996.

[2] Y. Tang and L. Xu, “Flexible active and reactive power control strategy for a variable speed constant frequency generating system,” IEEE Trans. Power Electron., vol. 10, no. 4, pp. 472–478, Jul. 1995.

[3] S. Peresada, A. Tilli, A. Tonielli, “Indirect stator flux-oriented output feedback control of a doubly fed induction machina”, *IEEE Transactions on Control Systems Technology*, vol. 11, no. 6, pp. 875-888, November 2003.

[4] G. Yuan; J. Chai; Y. Li, “Vector control and synchronization of doubly fed induction wind generator system”, IPEMC 2004, Volume 2, 14-16 Aug. 2004 pp. 886 - 890. August 14-16, 2004, Xi'an, China.

[5] A.G. Abo-Khalil, D-C Lee, S-H Lee, “Grid connection of doubly-fed induction generators in wind energy conversion system”, IPEMC 2006, Vol. 3, 14-16 Aug. 2006, pp. 1 - 5. August 14-16, 2006, Xi'an, China.

[6] V. Kaura, V. Blasko, “Operation of a Phase Locked Loop System under distorted Utility Conditions”, IEEE Transactions on Industry Applications, Vol. 33, n. 1, pp. 58-63, January/February 1997.